Journal of Applied Polymer Science

WILEY

Applied Polymer SCIENCE

RESEARCH ARTICLE OPEN ACCESS

Impact of Aluminum Diethyl Phosphinate (DEPAL) Flame Retardant on the Thermal, Mechanical, and Fire-Resistance Properties of an Amine-Cured Epoxy Resin

Max Friedel | Johanna Veronika Boehm | Holger Ruckdaeschel

Department of Polymer Engineering, University of Bayreuth, Bayreuth, Germany

Correspondence: Holger Ruckdaeschel (holger.ruckdaeschel@uni-bayreuth.de)

Received: 5 December 2024 | **Revised:** 6 February 2025 | **Accepted:** 11 February 2025

Funding: This work was supported by the German Bavarian Aviation Research Program BayLu25-AZA supported by the project sponsor IABG (Industrieanlagen-Betriebsgesellschaft mbH) and funded by the Bavarian State Ministry of Economic Affairs, Regional Development and Energy within the Research Project LargeDuroPrint—Großvolumiger Duromerer 3D-Druck für die Luftfahrt (Grant # ROB-2-3410.20-04-10/BLU-2109-0010).

ABSTRACT

Epoxy resin systems are widely used in industrial applications due to their excellent mechanical and thermal properties. However, their inherent flammability restricts use in safety-critical environments. To improve flame retardance, phosphorus-based additives like aluminum diethyl phosphinate (DEPAL) are commonly used. This study focuses on evaluating the effectiveness of DEPAL in the form of the commercial particulate additive OP935 as a flame retardant in a fast amine-curing epoxy resin system, EPIKOTE 06150. The incorporation of DEPAL significantly improves the flame retardance of the epoxy system, as evidenced by a reduced heat release rate and the Petrella plot. While OP935 improves flame retardance, its effects on other properties of the epoxy, such as mechanical strength and thermal stability, are also investigated. The results indicate that DEPAL may cause some reduction in flexural strength but does not negatively affect the thermal stability or glass transition temperature of the epoxy resin system. This balance between improved flame retardance and retained thermal properties suggests that DEPAL is a promising additive for the production of safer, more resilient epoxy resin systems suitable for various high-demanding performance applications such as aerospace.

1 | Introduction

Epoxy resin systems are used in a variety of industrial processes. Their main area of application is in the field of coatings, adhesives, sealants, or resin infusion for the production of composite materials [1, 2]. However, the kinetics of the curing is highly dependent on the curing temperature [3]. With this factor and the fitting curing agent, the properties of rapid, thermally induced curing can also be utilized for extrusion-based additive manufacturing [4]. This processing method has the potential to combine the advantages of large-area additive manufacturing with the outstanding thermomechanical properties of thermosets. One application area where the lightweighting potential of additive manufacturing is beneficial is the aerospace sector. It can be assumed that a reduction in weight by 1 kg leads to an annual saving of around 3000 € per aircraft, simply through the reduction in kerosene and the corresponding reduction in carbon emissions [5]. The additive manufacturing of epoxy resins is mainly used in civil aviation for optical and less safety-critical components. In contrast, metals are already being used for secondary structures or propulsion components. A major factor that is currently still hampering the use of additively manufactured polymers in safety-critical aircraft components is the lack of flame retardance and the lack of confidence in mechanical properties [5–7].

To reduce the flammability of epoxy resins, a large number of flame retardants are available, which can be categorized

according to their mode of action in the solid phase or the gas phase [8]. An alternative approach is to classify the additives according to their chemical properties. Examples include halogen compounds, metal hydroxides, and phosphorus-containing flame retardants [9]. Halogen compounds are increasingly being banned and withdrawn from the market as they have a carcinogenic and toxic effect [10, 11]. In this context, metal hydroxides can be considered uncritical, although a high loading of 30–40 wt% is required to achieve relevant effects [12]. Phosphorus-containing flame retardants can be added to the epoxy system both as reactive and additive substances. For example, reactive phosphorus-based flame retardants such as 9,10-dihydro-9-oxa-10-phosphaphenanthrene-10-oxide (DOPO) must react with the epoxy resins in order to be fully effective. Additive particulate materials such as red phosphorus, ammonium polyphosphate (APP) or aluminum diethyl phosphate (DEPAL) can be mixed into the resin mixture during the process [13–15].

The effectiveness of this subclass of flame retardants depends to a large extent on the proportion of phosphorus in the overall mixture. Significant effects can be expected starting from a phosphorus content of 2% by weight [16–19]. The mode of action of phosphorus-based flame retardants can be observed in both the gas and solid phases. The vast majority of phosphorus-based flame retardants cause a favorable change in the pyrolytic combustion path of plastics. This manifests itself, for example, in the formation of char or intumescent layers. In addition, phosphorus-based flame retardants can reduce the formation of gases, preventing further combustion. The decomposition products containing phosphorus also have an extinguishing effect on the flame [20]. Overall, DEPAL additives fulfill the most important properties for modern flame retardants. Other advantages include high effectiveness and cost-effective use [21].

The addition of flame retardants leads to a modification of the characteristics of the starting material with regard to thermal, mechanical, and fire protection aspects. In the context of thermal properties, an influence of DEPAL additives on the material decomposition temperature and the glass transition temperature can be observed. In thermogravimetric tests, Rabe et al. [22] demonstrated a small impact of DEPAL on epoxy resin systems. The observation of an earlier initial decomposition with increasing additive addition can be explained by the catalytic effect, which promotes the formation of free radicals and thus reduces the activation energy of the decomposition [22]. The slightly changed decomposition temperatures with a mass loss of 5% allow the conclusion that the flame retardant has good integrity in the system. An analysis of the glass transition temperatures shows that DEPAL has a neutral to positive effect on epoxy resin systems. In the study by Gu et al. [23], an increase in the glass transition temperature in the epoxy resin system from 148°C to 154°C is observed, although the reason is not stated.

Regarding mechanical performance, the use of DEPAL in epoxy resins has a twofold effect, as described by Liu et al. [24] On the one hand, the addition of 20% by weight of flame retardant additive increases the matrix stiffness and reduces matrix deformability, which leads to a slight increase in flexural stiffness of 10%. On the other hand, a strong decrease of the bending stiffness by 26% can be observed with the same weight percentage of additive, as the incorporation of the particles acts levels to microcrack formation and thus reduces the overall strength of the system. A similar study by Liu et al. [25] also showed a decrease in flexural strength from 95 to 68 MPa with the same weight load of the DEPAL agent OP930. At the same time, however, a reduction in flexural modulus of approx. 16% was also observed. In particular, the agglomeration of the highly polar phosphorus-containing flame retardants and air inclusions should be avoided when adding particulate additives, as these result in a further deterioration of the mechanical properties of the material. The use of low-viscosity materials or a vacuum for high-viscosity formulations can help here [21].

In their study of fire properties, Rabe et al. [22] analyzed various DEPAL loadings in the cone calorimeter and observed a continuous improvement in the time to ignition (t_{ig}), the peak heat release rate (*p*HRR), the total heat release rate (THRR) and the char residue due to the successive addition of flame retardant. The greatest improvements were observed at DEPAL loadings of 10 wt% (corresponding to 2 wt% phosphorus). A further increase in loading resulted only in slight improvements. As the phosphorus content increased, an increase in the char layer was observed. The formation of a char layer on the surface of the polymer has an insulating effect and protects it from further heat and oxygen, which serve as "fuel" for the flame during combustion. Furthermore, UL94 tests were carried out to determine the flame retardance class of DEPAL epoxy resin combinations. The classifications range from a V-0 rating with 15 wt% loading and a 3 mm sample thickness to a V-0 rating with 9.5 wt% loading without specifying the sample thickness [18, 26]. In the publications on the subject of flame retardance, the substance Exolit OP935 from Clariant is mentioned, which is a widely used particulate additive for the production of flame-retardant properties [18].

While numerous publications have examined the influence of DEPAL on epoxy resins, they often focus on isolated aspects without considering other parameters. This study aims to simultaneously analyze the three key pillars:

a. thermal properties;
b. mechanical properties; and
c. flame retardant properties

using a fast-curing DEPAL epoxy resin combination and to use widely recognized and state of the art experimental methods to create the basis for a raw material that has the potential to be processed using large-scale extrusion printing and thermally induced curing. The aim is to gain an understanding of the effects of flame retardant loading.

2 | Experimental

2.1 | Materials

The resin system EPIKOTE Resin TRAC 06150 and the amine curing agent EPIKURE Curing Agent TRAC 06150 were kindly provided by Westlake Epoxy Inc. (Waalwijk, the Netherlands). The particle DEPAL flame retardant EXOLIT OP935 has been acquired from Clariant AG (Frankfurt am Main, Germany). It has a pure phosphorus content of approximately 24% by weight.

2.2 | Resin Formulation

A total of five mixtures are produced, whereby one mixture is prepared as a neat system without a flame retardant additive and four further mixtures with increasing flame retardant content (see Table 1). The quantities of OP935 added are given 'on top' of the pure resin system, which corresponds to the common term phr (parts per hundred rubber).

Before mixing the resin with the hardener, the resin is preheated to 60°C in the oven for 20 min in order to reduce viscosity. In the case of the NEAT system, the resin and hardener are mixed at a weight ratio (100:24) in a speed mixer (Hauschild GmbH & Co. KG, Hamm, Germany) at 2000 rpm for 4 min. In the case of samples loaded with flame retardant, the OP935 is first mixed with the preheated resin at 2000 rpm for 4 min and then placed back in the oven at 60°C for 20 min. This is followed by mixing with the hardener and repeated mixing in the speed mixer at 2000 rpm for 4 min. After this process, the formulation is poured into closed molds.

2.3 | Curing and Sample Preparation

A temperature program is set for oven curing the samples. The epoxy systems are heated from 25°C to 150°C within 30 min. Subsequently, a temperature of 150°C is maintained for 90 min, followed by cooling down to 25°C within 30 min. This temperature ramp, which is very slow for the system, ensures that curing in the closed molds is as gentle and complete as possible. The cured samples are then cut to their size and thickness using a diamond table saw (Diadisc 6200, Mutronic GmbH & Co. KG, Rieden am Forggensee, Germany) and a disc grinding machine (RotoPol-21, Struers GmbH, Willich, Germany) with P80 abrasive paper and a force of 15 N at 300 rpm.

2.4 | Material Characterization

2.4.1 | Thermal Properties

2.4.1.1 | Dynamic Mechanical Analysis (DMA). The glass transition temperature (T_g) was determined by means of dynamic mechanical analysis in shear mode under oscillatory loading. Three specimens with dimensions of $50 \times 10 \times 2\,mm^3$ are analyzed. The test specimens are tested with an oscillating deformation of 0.1% and a frequency of 1 Hz at a heating rate of 10 K/min from 25°C to 170°C. The Rheometric Scientific RDA III from TA Instruments (New Castle, USA) is used as the test device. The storage modulus (G') and loss modulus (G'') are determined during dynamic mechanical analysis. The loss modulus (G'') reflects the viscous response of the material, where energy is dissipated rather than elastically stored and returned. This dissipation is due to the viscoelastic nature of the material, resulting from molecular relaxation processes at the applied temperature. The ratio of storage modulus to loss modulus is known as the loss factor tan δ, which is indicating the T_g when reaching its maximum [27]:

$$\tan\,\delta = \frac{G''}{G'} \tag{1}$$

2.4.1.2 | Thermogravimetric Analysis (TGA). Analyzing the fully cured samples by TGA provides insight into their thermal stability. The analysis is carried out on the TG 209 F1 Libra (Erich NETZSCH B.V. & Co. Holding KG, Selb, Germany) at a heating ramp of 10 K min^{-1} and a temperature range of 25°C–800°C. The measurement is performed in a synthetic air atmosphere with a flow rate of 250 mL min^{-1}. The temperatures at which 2% relative mass loss ($T_{\Delta 2\%}$) and 5% relative mass loss ($T_{\Delta 5\%}$) occur are determined as characteristic values. Three samples are tested per material. The mean value and its standard deviation are provided.

2.4.2 | Mechanical Properties

2.4.2.1 | Three-Point Bending Test (3PB). To evaluate flexural strength (σ_f), flexural modulus (E_f), and maximum deflection to failure (ε_f), five $80 \times 10 \times 4\,mm^3$ bending specimens were analyzed in accordance with ASTM D790. Flexural strength (σ_f) is the maximum stress a material can withstand in bending before failure, indicating its resistance to deformation under a bending load. The flexural modulus (E_f) represents the stiffness of the material in bending, and the maximum deflection to failure (ε_f) is the strain at which the specimen fails. The tests were performed on the zwickiLine 2.5 from ZwickRoell (Ulm, Germany).

2.4.2.2 | Charpy Impact Strength. Notched impact strength is tested in accordance with the instrumented impact test standard DIN EN ISO 179-2. One set consists of five specimens with dimensions of $80 \times 10 \times 3\,mm^3$ with a lateral A-notch depth of 2 ± 0.2 mm. The tests are carried out on the RKP 5114 from ZwickRoell (Ulm, Germany). The measured impact strength in kJ m^{-2} represents the toughness of a material.

2.4.3 | Flame Retardant Properties

2.4.3.1 | UL94 Test. To evaluate the flame retardant properties, the vertical UL94 test is carried out in accordance with DIN EN 60695-11-10 with a 20 mm (50 W) flame. The sample dimensions are $125 \times 13 \times 3$ and $125 \times 13 \times 2\,mm^3$, respectively. The thickness of the test samples determines the minimum thickness required for the final part. As part of the experiment, the samples are flamed at a 45° angle for a period of 10 s, after which the duration of burning (t_1) is determined. If the flame does not burn through to

TABLE 1 | Resin formulations.

Formulation name	Addition of OP935 (wt%)	Phosphorus content in the total system (wt%)
NEAT	0%	0
5% OP935	5%	1.14
10% OP935	10%	2.18
15% OP935	15%	3.13
20% OP935	20%	4.00

the clamp, a further flame is applied for a period of 10 s, followed by the measurement of the burning time t_2. As the tested samples do not show any afterglow, $t_3 = 0$. The calibration of the flame was checked in accordance with the applicable standards using a thermocouple, a stopwatch, and a metal ruler. The flame retardance is classified according to Table 2.

2.4.3.2 | Cone Measurements. Cone calorimetry supplements UL94 tests by a measurement method involving continuous heat exposure. The tests are carried out in accordance with the standard ISO 5660-1: 2015-03. As part of a series of tests, three square samples measuring $100 \times 100 \times 3\,mm^3$ are placed one after the other on a scale and uniformly irradiated with heat radiation of $35\,kW\,mm^{-2}$ by a conical heating coil. The process described here requires forced combustion, in which the pyrolysis gases are ignited using an external spark generator, also known as a spark igniter. The resulting combustion gases are then passed through various analyzers. Before the start of each new series of measurements, the flue gas flow, the gas analyzers, and the radiant heater are calibrated. The heat release rate (HRR) is calculated over time, taking into account the oxygen content and the flue gas volume flow. The analysis of the curves allows one to derive the characteristic fire behavior of the materials. The THRR is calculated by integrating the time-dependent curve of the HRR. Table 3 lists the main parameters documented during the tests [28, 29].

To determine quantitative statements regarding the rate of spread and the heat release potential of a fire, the fire growth index is calculated according to Petrella, as shown in Formula 2, and its graphical representation in a diagram as a function of the total heat release rate [30]:

$$\text{Fire growth index} = \frac{p\text{HRR}}{t_{ig}} \quad (2)$$

Figure 1 illustrates the significance of the so-called Petrella plot. The *y*-axis shows the THRR, which provides information about the intensity of the fire. The *x*-axis shows the fire growth index, which describes the rate of spread. The figure can be explained as follows: values in the upper right quadrant are classified as burning fast and hot, while values in the lower left quadrant are classified as slow and comparatively cool. The aim is to minimize the propagation speed and heat release at the same time [29].

TABLE 2 | Qualification criteria for UL94 according to DIN EN 60695-11-10.

Criterium	V-0	V-1	V-2
Burn-through to the clamp	No	No	No
Drops ignite cotton wool	No	No	Yes
t_1 or t_2	10 s	30 s	30 s
$t_2 + t_3$	30 s	60 s	60 s
$\sum (t_1 + t_2)$	50 s	250 s	250 s

3 | Results and Discussion

3.1 | Thermal Properties

3.1.1 | Dynamic Mechanical Analysis (DMA)

The dynamic mechanical and thermogravimetric properties, both shown in Figure 2 and Table 4, show consistent behavior. It can be seen that the loss factor decreases continuously with the

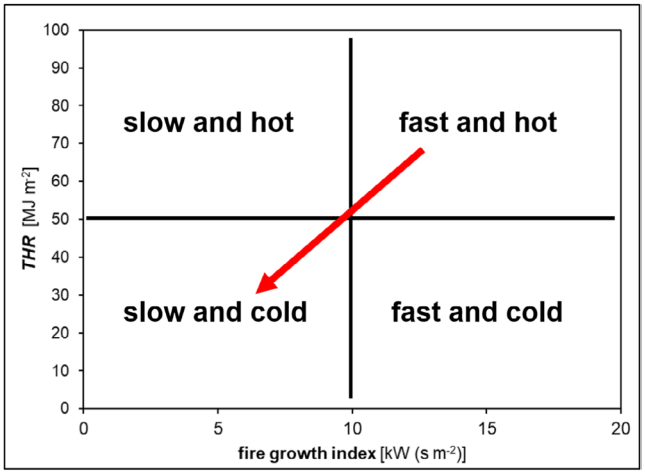

FIGURE 1 | Schematic representation of the Petrella plot based on Schartel and Hull and the desired direction of improvement [29]. [Color figure can be viewed at wileyonlinelibrary.com]

TABLE 3 | Determined values of the cone measurements.

Measured value	Designation	Explanation
Time to ignition	t_{ig} [s]	Time until ignition of the sample
Heat release rate	HRR [$kW\,m^{-2}$]	Amount of heat released in relation to the sample surface per time unit
Peak heat release rate	pHRR [$kW\,m^{-2}$]	Maximum value of the heat release rate
Total heat release rate	THRR [$MJ\,m^{-2}$]	Total amount of heat released in relation to to the sample surface
Total smoke release	TSR [$m^2\,m^{-2}$]	Total smoke release in relation to the sample surface
Residue	[%]	Relative mass of the burnt residue

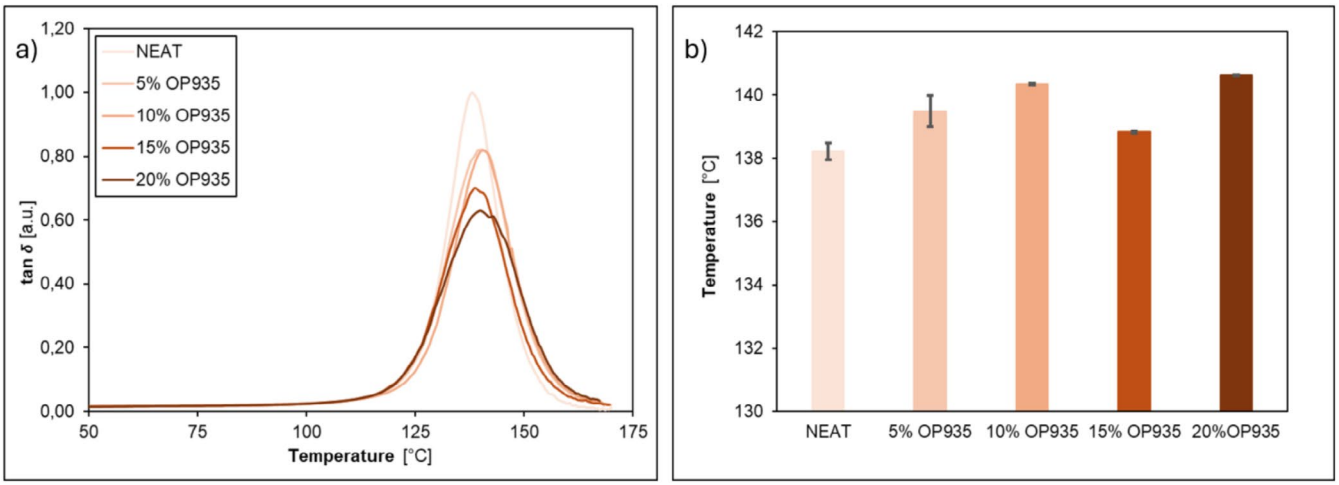

FIGURE 2 | DMA results of (a) loss factor (b) glass transition temperature. [Color figure can be viewed at wileyonlinelibrary.com]

TABLE 4 | Results of the thermal analyses.

Sample name	T_g (°C)	$T_{2\%}$ (°C)	$T_{5\%}$ (°C)	Residue mass (%)
NEAT	138 ± 1	302 ± 2	339 ± 2	0 ± 0
5% OP935	140 ± 1	299 ± 7	338 ± 4	1 ± 1
10% OP935	140 ± 0	292 ± 3	332 ± 4	5 ± 0
15% OP935	139 ± 0	296 ± 10	333 ± 6	7 ± 0
20% OP935	140 ± 0	290 ± 9	331 ± 7	9 ± 1

addition of OP935, while T_g is hardly affected, with an overall increase of 2°C (from 138°C to 140°C) being the standard deviation. These results confirm that the addition of OP935 has a neutral to slightly positive effect on the glass transition temperature, which can be attributed to the increased catalytic effect in resin curing [23]. Overall, the modification with OP935 results in a flatter and broader curve. This can be confirmed by analyzing the full width at half maximum of the T_g, which increases from 13 to 21 K (equaling an increase of 62%) indicating that the network becomes more heterogeneous with increasing flame retardant content [31].

3.1.2 | Thermogravimetric Analysis (TGA)

The evaluation of the TGA results in Figure 3 and Table 4 shows a consistent picture. The addition of OP935 causes a moderate but continuous drop in the decomposition onset temperature $T_{2\%}$ from 302°C to 290°C. The addition of OP935 leads to a slightly earlier decomposition of the resin system due to acid-catalyzed epoxy ring opening. OP935 releases phosphorus compounds, which open the epoxy rings of the resin and thus cause the polymer chains to become unstable prematurely [22, 32]. At a temperature at which a mass loss of 5% is recorded, the difference between NEAT and 20% OP935 is similar, with a reduction of 8°C. The $T_{2\%}$ and $T_{5\%}$ values of the NEAT resin are in a similar range to those of the modified systems, indicating that the thermal degradation behavior of the polymer remains largely unchanged with the addition of the

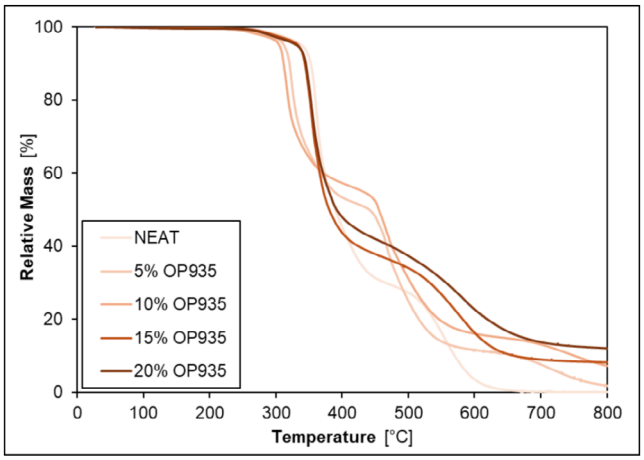

FIGURE 3 | TGA curves of the formulations. [Color figure can be viewed at wileyonlinelibrary.com]

flame retardant. This indicates that the flame retardant is well integrated into the polymer matrix without significantly altering its thermal degradation properties. If the flame retardant were poorly dispersed or poorly compatible, phase separation, localized degradation, or significant shifts in TGA values could occur due to altered decomposition pathways. The observed similarity in $T_{2\%}$ and $T_{5\%}$ indicates that the flame retardant is interacting effectively with the polymer, maintaining a uniform structure and ensuring stable thermal performance in both the modified and unmodified systems [33]. In addition, a $T_{2\%}$ of 290°C excludes the effect of unintentionally incorporated water in the form of physically bound water and hydrophilic by-products, which would be amplified in the temperature range of 90°C–200°C [34]. As a result of enhanced charring caused by the increased phosphorus content, the samples containing flame retardants exhibit higher residues at the end of the TGA curves [22]. In addition, the curves with 15% OP935 and 20% OP935 show a steeper drop in relative mass in the first decomposition stage between 300°C and 400°C, with the main decomposition between 400°C and 600°C proceeding more slowly. The reason for the first steeper drop at the first decomposition stage relates to the main degradation of the flame retardant OP935, which takes place between 350°C and 400°C and matches the first decomposition stage of the NEAT system [18]. The flattening of

the second decomposition stage is due to the already reacted flame retardant mass in the mixture.

3.2 | Mechanical Properties

3.2.1 | Three-Point Bending Test (3 PB)

The addition of the particulate flame retardant leads to a significant deterioration in flexural strength. While the σ_f without flame retardant is 117 MPa, it is only 64 MPa with 20 wt% flame retardant. This corresponds to a reduction of 53%. Implementation of the flame retardant therefore leads to a negative influence on the mechanical strength. At a high load, inhomogeneous distribution can serve as a starting point for microcracks and can therefore lead to weak points in the system [24, 35, 36]. Values for ε_f are shown in Table 5 illustrating the negative influence on the bending mechanics. At a maximum loading of 20% by weight, the elongation at break drops from 6% to 3%. Noteworthy is the initial drop in mechanical properties at 5% loading and only a slight impairment when further increasing loading. The E_f values in Table 5 and Figure 4 show a reduction of approx. 10% when adding flame retardants.

TABLE 5 | Results of the mechanical tests.

System	E_f (GPa)	σ_f (MPa)	ε_f (%)	(kJ m^{-2})
NEAT	2.6 ± 0.4	117 ± 14	6.3 ± 0.8	0.8 ± 0.2
5% OP935	2.4 ± 0.3	77 ± 24	3.5 ± 1.0	0.8 ± 0.1
10% OP935	2.1 ± 0.5	68 ± 14	3.6 ± 0.4	1.0 ± 0.3
15% OP935	2.2 ± 0.3	58 ± 12	2.7 ± 0.4	0.8 ± 0.2
20% OP935	2.4 ± 0.3	64 ± 10	3.1 ± 0.8	1.0 ± 0.3

3.2.2 | Notched Impact Strength According to Charpy

The addition of the flame retardant does neither diminish nor improve the values within the high standard deviation. Figure 5 shows that the addition of OP935 has no significant effect on embrittlement or toughening in Charpy tests, as OP935 is unlikely to significantly affect the energy absorption capacity or toughness of the matrix, both of which are critical to impact strength.

3.3 | Flame Retardant Properties

3.3.1 | Cone Measurements

The measured HRR curves are shown in Figure 6a. A sharp peak for the NEAT system is observed, which is considered characteristic of rapid combustion. After reaching the maximum, all curves show a steep drop, followed by a clear leveling off. This behavior is characteristic of materials with a tendency for low to medium residue formation [29]. A lower HRR curve can be observed for the flame-retardant samples, peaking at similar firing times to the non-flame-retarded samples. The addition of the flame retardant results in a minor delay in t_{ig}. For 20 wt% OP935, the fire starts after 82 s, which corresponds to a delay of 11 s compared to the pure resin system.

The *p*HRR clearly decreases with flame retardant and phosphorus content. For example, the heat release drops to 550 kW m^{-2}, by adding 20 wt% of OP935, while the NEAT system, in contrast, shows almost double the energy release at 1094 kW m^{-2}. The same tendencies can also be seen when looking at the THR of 20% OP935, which drops by 30% to 68 MJ m^{-2}. With increasing phosphorus loading, the formation of PO radicals increases, which act as radical scavengers and thus significantly inhibit the combustion process [37]. The gas-phase reaction induces incomplete

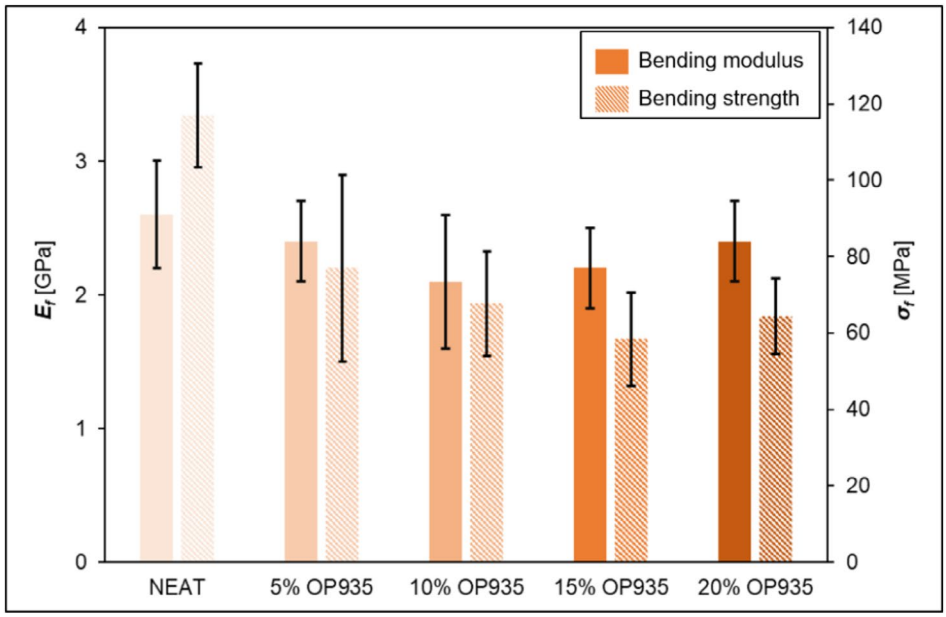

FIGURE 4 | Bending modulus values and bending strengths of the three-point bending tests. [Color figure can be viewed at wileyonlinelibrary.com]

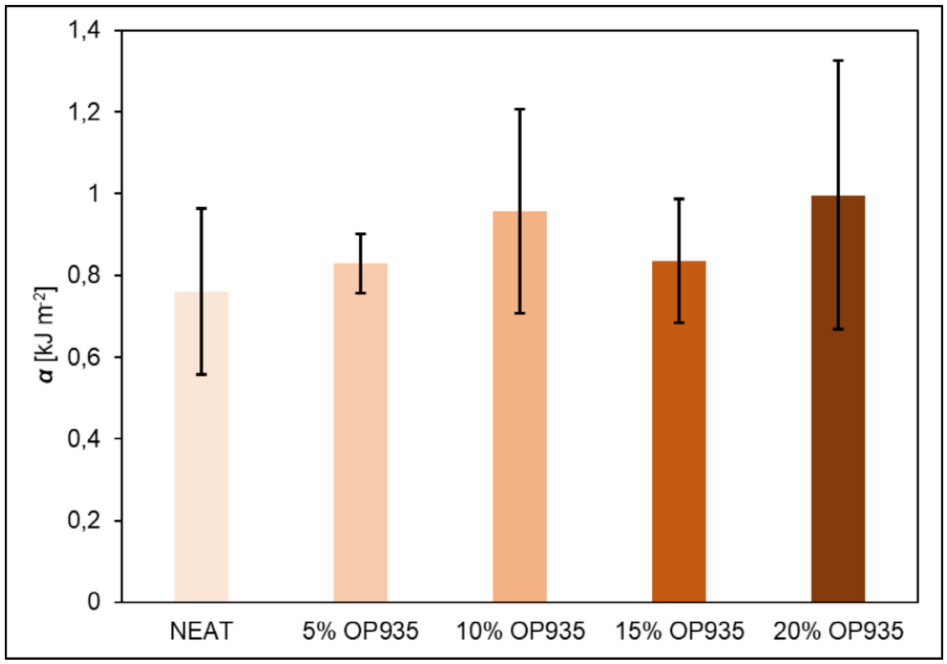

FIGURE 5 | Notched impact strength according to Charpy. [Color figure can be viewed at wileyonlinelibrary.com]

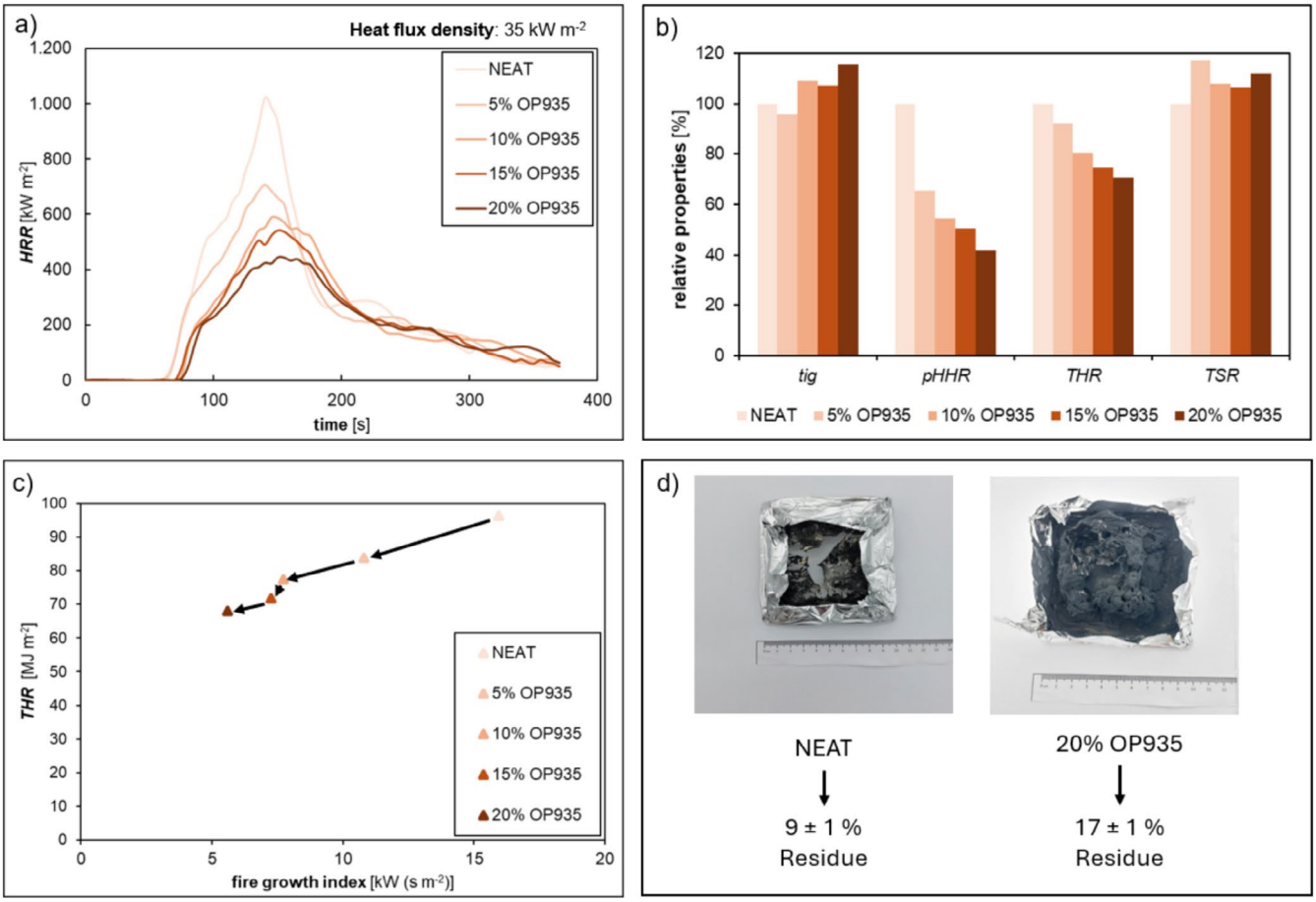

FIGURE 6 | Cone measurements: (a) HRR (b) relative properties (c) Petrella plot (d) samples and their residues after testing. [Color figure can be viewed at wileyonlinelibrary.com]

TABLE 6 | Results of the flame retardant properties.

	UL94		Cone				
System	**3 mm**	**2 mm**	t_{ig} **(s)**	***p*HRR (kW m^{-2})**	**THR (MJ m^{-2})**	**TSR (m^2 m^{-2})**	**Residue (%)**
NEAT	FAIL	FAIL	71 ± 13	1094 ± 75	96 ± 1	3319 ± 82	9 ± 1
5% OP935	FAIL	V2	68 ± 11	717 ± 33	88 ± 7	3888 ± 255	11 ± 2
10% OP935	V0	V1	77 ± 1	594 ± 48	77 ± 2	3578 ± 141	17 ± 5
15% OP935	V0	V0	75 ± 4	550 ± 45	72 ± 5	3532 ± 106	17 ± 3
20% OP935	V0	V0	82 ± 3	457 ± 25	68 ± 2	3717 ± 48	17 ± 1

combustion, which leads to a slight increase in the total smoke release [29]. In the solid phase, aluminum diethyl phosphinate undergoes thermal decomposition, releasing phosphoric acid and phosphorus-containing species that promote the formation of an intumescent char layer. This char acts as a physical barrier, slowing heat transfer and limiting the availability of oxygen to the underlying polymer. As a result, cone calorimeter measurements show an increased residual mass of 17% (20% OP935) compared to 9% (NEAT), which is in good agreement with the TGA results. Figure 6d compares two exemplary samples to show the pronounced formed char with flame retardant loading [22].

The greatest effects in relation to the load occur at 10% OP935. The fastest percentage improvement in the values t_{ig}, *p*HRR, THR, and TSR can be seen in Figure 6b. A further increase results in positive effects in the area of flame retardance, but these are only slight.

When using the Petrella plot (Figure 6c), an improvement in the fire growth index and total heat release is achieved by increasing the total phosphorus content. In particular, the formulations with 5 and 10 wt% OP935 reduce the risk of a fast-growing fire most effectively. The probability of a long-lasting fire (THR) is also reduced by the addition of a flame retardant additive, whereby the fire growth index is reduced to a greater extent.

3.3.2 | UL94 Test

The results of the UL94 test, as summarized in Table 6, show that the pure resin system without flame retardants fails the test as the test bars burn completely. However, as the phosphorus content increases, the fire performance improves significantly. Even a small addition of 5% by weight OP935 is sufficient to achieve a UL94-V2 classification at 3 mm. By increasing the loading to 15% by weight (3.13% phosphorus) and 20% by weight (4.00% phosphorus), the highest classification V-0 is achieved for a sample thickness of 2 mm. Thickness plays a crucial role here as thicker samples dissipate heat more effectively, delaying ignition and improving the UL94 classification [38]. Overall, the results of the UL94 test correlate very well with the results of the Cone measurement.

4 | Summary and Conclusion

In this work, the influence of a phosphorus-based DEPAL flame retardant OP935 on the thermal, mechanical, and flame retardant properties in combination with a fast-curing epoxy resin was investigated. Increasing the amount of OP935 showed no significant change in $T_{2\%}$, $T_{5\%}$, or T_g. The mechanical properties were significantly compromised in terms of σ_f as a consequence of the additive loading. This was attributable to the introduction of weak points in the system, serving as starting points for failure. The notched impact strength was not significantly changed by the additives. In terms of flame retardant properties, 10 wt% OP935 loading already showed significant results such as slower spread of fire, reduction in heat release, and also passing the UL94 test at 3 mm. A further increase in the flame retardant load only led to marginally better effects, such as a slightly reduced *p*HRR in the cone test or a V-0 rating at 2 mm specimen thickness.

The combination of OP935 with an amine-curing epoxy resulted in a system that exhibits favorable thermal and flame retardant properties in conjunction with amine curing. The system displays a high T_g and reliable flame retardant properties, which render it particularly promising for resin-based additive manufacturing, including in the civil aviation sector.

Author Contributions

Max Friedel: conceptualization (lead), data curation (lead), investigation (lead), methodology (lead), supervision (equal), validation (lead), visualization (lead), writing – original draft (lead), writing – review and editing (lead). **Johanna Veronika Boehm:** conceptualization (supporting), data curation (equal), investigation (supporting), methodology (supporting), validation (equal), visualization (equal). **Holger Ruckdaeschel:** funding acquisition (lead), project administration (lead), supervision (lead), writing – review and editing (equal).

Acknowledgments

We would like to thank all colleagues of the work group "Resins and composites" at the Department of Polymer Engineering for their support. Open Access funding enabled and organized by Projekt DEAL and the Open Access Publishing Fund of the University of Bayreuth.

Conflicts of Interest

The authors declare no conflicts of interest.

Data Availability Statement

The data that support the findings of this study are available from the corresponding author upon request.

References

1. C. R. Wang, Y. Z. Gu, K. M. Zhang, M. Li, and Z. G. Zhang, "Rapid Curing Epoxy Resin and Its Application in Carbon Fibre Composite

Fabricated Using Vartm Moulding," *Polymers and Polymer Composites* 21 (2013): 315–324.

2. I. Hamerton and I. Hamerton, *Recent Developments in Epoxy Resins* (iSmithers Rapra Publishing, 1996).

3. A. Yousefi, P. G. Lafleur, and R. Gauvin, "Kinetic Studies of Thermoset Cure Reactions: A Review," *Polymer Composites* 18 (1997): 157–168.

4. S. Romberg, C. Hershey, J. Lindahl, W. Carter, B. Compton, and V. Kunc, "SAMPE 2019", https://doi.org/10.33599/nasampe/s.19.1616.

5. S. Singanmneni, Y. LV, A. Hewitt, R. Chalk, W. Thomas, and D. Jordison, "Additive Manufacturing for the Aircraft Industry: A Review," *Journal of Aeronautics and Aerospace Engineering* 8, no. 1 (2019): 215, https://doi.org/10.35248/2168-9792.19.8.215.

6. Y.-C. Wang, T. Chen, and Y.-L. Yeh, "Advanced 3D Printing Technologies for the Aircraft Industry: A Fuzzy Systematic Approach for Assessing the Critical Factors," *International Journal of Advanced Manufacturing Technology* 105 (2019): 4059–4069.

7. M. Hinsch and J. Olthoff, eds., *Impulsgeber Luftfahrt* (Springer Berlin Heidelberg, 2013).

8. P. R. Hornsby, "Fire Retardant Fillers for Polymers," *International Materials Reviews* 46 (2001): 199–210.

9. J. Troitzsch and E. Antonatus, eds., *Plastics Flammability Handbook: Principles, Regulations, Testing, and Approval* (Hanser, 2021).

10. S. D. Shaw, A. Blum, R. Weber, et al., "Halogenated Flame Retardants: Do the Fire Safety Benefits Justify the Risks?," *Reviews on Environmental Health* 25 (2010): 261–305.

11. S. Kemmlein, D. Herzke, and R. J. Law, "Brominated Flame Retardants in the European Chemicals Policy of REACH—Regulation and Determination in Materials," *Journal of Chromatography A* 1216 (2009): 320–333.

12. W. Xiao, P. He, G. Hu, and B. He, "Study on the Flame-Retardance and Thermal Stability of the Acid Anhydride-Cured Epoxy Resin Flame-Retarded by Triphenyl Phosphate and Hydrated Alumina," *Journal of Fire Sciences* 19 (2001): 369–377.

13. X. Chen, J. Wang, S. Huo, S. Yang, B. Zhang, and H. Cai, "Study on Properties of Flame-Retardant Cyanate Esters Modified With DOPO and Triazine Compounds," *Polymers for Advanced Technologies* 29 (2018): 2574–2582.

14. G. Liu, *4th International Conference on Bioinformatics and Biomedical Engineering* (IEEE, 2010).

15. M. Ciesielski, B. Burk, C. Heinzmann, and M. Döring, *Novel Fire Retardant Polymers and Composite Materials. Number 73*, ed. D.-Y. Wang (Elsevier/WP, Woodhead Publishing, 2017), 3–51.

16. B. Schartel, "Phosphorus-Based Flame Retardancy Mechanisms—Old Hat or a Starting Point for Future Development?," *Materials* 3 (2010): 4710–4745.

17. C. H. Lin, "Synthesis of Novel Phosphorus-Containing Cyanate Esters and Their Curing Reaction With Epoxy Resin," *Polymer* 45 (2004): 7911–7926.

18. M. Rakotomalala, S. Wagner, and M. Döring, "Recent Developments in Halogen Free Flame Retardants for Epoxy Resins for Electrical and Electronic Applications," *Materials* 3 (2010): 4300–4327.

19. T. Neumeyer, "Struktur und Eigenschaften Neuer, Flammgeschützter Prepreg-Matrixsysteme für Anwendungen in der Kabine von Verkehrs-Flugzeugen," 2015 Bayreuth.

20. Y. F. Lv, W. Thomas, R. Chalk, and S. Singamneni, "Flame Retardant Polymeric Materials for Additive Manufacturing," *Materials Today Proceedings* 33 (2020): 5720–5724.

21. R.-D. Maier and M. Schiller, *Handbuch Kunststoff Additive* (Carl Hanser Verlag GmbH & Co. KG, 2016).

22. S. Rabe, Y. Chuenban, and B. Schartel, "Exploring the Modes of Action of Phosphorus-Based Flame Retardants in Polymeric Systems," *Materials* 10 (2017): 455.

23. L. Gu, J. Qiu, and E. Sakai, "Thermal Stability and Fire Behavior of Aluminum Diethylphosphinate-Epoxy Resin Nanocomposites," *Journal of Materials Science: Materials in Electronics* 28 (2017): 18–27.

24. X. Liu, J. Liu, and S. Cai, "Comparative Study of Aluminum Diethylphosphinate and Aluminum Methylethylphosphinate-Filled Epoxy Flame-Retardant Composites," *Polymer Composites* 33 (2012): 918–926.

25. X. Liu, J. Liu, S. Sun, and J. Chen, "A New Type of Flame Retarded Epoxy Resin Based on Metal Phosphinates," *Polymers and Polymer Composites* 20 (2012): 151–154.

26. Q. Liu, D. Wang, Z. Li, et al., "Recent Developments in the Flame-Retardant System of Epoxy Resin," *Materials* 13 (2020): 2145.

27. K. P. Menard and N. R. Menard, *Dynamic Mechanical Analysis* (CRC Press, Taylor and Francis Group, 2020).

28. L. Greiner, P. Kukla, S. Eibl, and M. Döring, "Phosphorus Containing Polyacrylamides as Flame Retardants for Epoxy-Based Composites in Aviation," *Polymers* 11 (2019): 284.

29. B. Schartel and T. R. Hull, "Development of Fire-Retarded Materials—Interpretation of Cone Calorimeter Data," *Fire and Materials* 31 (2007): 327–354.

30. R. V. Petrella, "The Assessment of Full-Scale Fire Hazards from Cone Calorimeter Data," *Journal of Fire Sciences* 12 (1994): 14–43.

31. N. R. Manoj, R. D. Raut, P. Sivaraman, D. Ratna, and B. C. Chakraborty, "Sequential Interpenetrating Polymer Network of Poly(Ethyl Methacrylate) and Carboxylated Nitrile Rubber: Dynamic Mechanical Analysis and Morphology," *Journal of Applied Polymer Science* 96 (2005): 1487–1491.

32. L. A. Berben, "Catalysis by Aluminum(III) Complexes of Non-Innocent Ligands," *Chemistry—A European Journal* 21 (2015): 2734–2742.

33. C. S. Wu, Y. L. Liu, Y. C. Chiu, and Y. S. Chiu, "Thermal Stability of Epoxy Resins Containing Flame Retardant Components: An Evaluation With Thermogravimetric Analysis," *Polymer Degradation and Stability* 78 (2002): 41–48.

34. C. Chen, J. Luan, G. Ji, F. Lan, C. Dong, and Z. Lu, "Construction of a Durable, Halogen-Free, and Phosphorus-Free Flame Retardant Cotton Fabric System With Hydrophobic Properties by Phase Separation and Interface Polymerization," *International Journal of Biological Macromolecules* 278 (2024): 135059.

35. Y. Wang, D. Jiang, X. Wen, et al., "Investigating the Effect of Aluminum Diethylphosphinate on Thermal Stability, Flame Retardancy, and Mechanical Properties of Poly(Butylene Succinate)," *Frontiers in Materials* 8 (2021): 737749.

36. F. A. M. M. Gonçalves, M. Santos, T. Cernadas, P. Alves, and P. Ferreira, "Influence of Fillers on Epoxy Resins Properties: A Review," *Journal of Materials Science* 57 (2022): 15183–15212.

37. M. M. Velencoso, A. Battig, J. C. Markwart, B. Schartel, and F. R. Wurm, "Molecular Firefighting—How Modern Phosphorus Chemistry Can Help Solve the Challenge of Flame Retardancy," *Angewandte Chemie International Edition* 57 (2018): 10450–10467.

38. Y. Wang and J. Zhang, "Influences of Specimen Size and Heating Mode on the Ignitability of Polymeric Materials in Typical Small-Scale Fire Test Conditions," *Fire and Materials* 36 (2012): 231–240.